Collapse of Monolayers of 10,12-Pentacosadiyonic Acid: Kinetics and Structure

C. Gourier,*,† C. M. Knobler,‡ J. Daillant,§,|| and D. Chatenay⊥

Laboratoire de Physique Statistique de l'Ecole Normale Supérieure, 24 rue Lhomond, 75231 Paris Cedex 05, France; LURE, CNRS/CEA/MINREC, Bât. 209D, Centre Universitaire Paris-sud, 91898 Orsay Cedex, France; DSM/SPEC, CEA Saclay, 91191 Gif-sur-Yvette Cedex, France; Department of Chemistry and Biochemistry, University of California, Los Angeles, California 90095-1569; and Laboratoire de Dynamique des Fluides Complexes, U.M.R. C.N.R.S. 7506, Strasbourg, France

Received June 27, 2002. In Final Form: September 9, 2002

The collapse of monolayers of 10,12-pentacosadiyonic acid at the air/water interface has been studied by measurements of isotherms as a function of temperature, compression speed, and spreading solvent. Films on the water surface have been examined by X-ray reflectivity, and atomic force microscopy (AFM) images have been obtained of films transferred to mica by the Langmuir−Blodgett method. At constant temperature, collapse occurs at constant pressure, which increases with the logarithm of the compression speed, suggesting an activation controlled process. Both the AFM and reflectivity measurements are consistent with the formation of a trilayer upon collapse. A mechanical model for collapse is discussed.

Introduction

Although there have been major advances in our understanding of phase transitions in Langmuir monolayers during the past decade, the process of collapse, the transition of a monolayer to a three-dimensional phase, remains poorly understood. The key imaging methods that have been essential to the study of Langmuir monolayers, Brewster-angle microscopy (BAM) and fluorescence microscopy, provide little direct information about the details of the structure of films normal to the interface. X-ray reflectivity and diffraction measurements, which have played a key role in determining the microscopic structure of monolayers, have not often been used to examine collapse.

Some of the earliest investigations of the mechanism of collapse were performed by Ries, who prepared Langmuir−Blodgett (LB) films of collapsing monolayers and imaged them by electron microscopy.[1] More recently, several groups have carried out similar experiments in which the topography of collapsed films was determined by atomic force microscopy (AFM). Birdi and Vu[2] transferred collapsed films of stearic acid spread on a $MgCl_2$ subphase to a pyrolitic graphite substrate. AFM images showed the presence of steps corresponding to monolayer, bilayer, and trilayer. Vollhardt et al.[3] prepared LB films of eicosanoic acid on glass cover slips. The AFM images show the presence of three-dimensional "micrograins" a few nanometers to tens of nanometers high. Similar structures have been found by AFM in collapsing monolayers of heneicosanoic acid.[4] The formation of multilayers in the collapse of poly(organosiloxane)s has also been followed by topographical imaging of LB films on mica.[5]

We are aware of only two previous X-ray studies of collapse at the air/water interface. Ibn-Elhaj et al.[6] performed X-ray reflectivity measurements of a three-block siloxane smectic liquid crystal on concentrated salt solutions. They were able to confirm that these films undergo successive layering transitions in bilayer steps, and they showed that beyond the monolayer the thickness of the film was consistent with that of the bulk smectogen. Grazing incidence diffraction (GIXD) measurements on compressed monolayers of cholesterol have revealed the formation of a crystalline phase about two layers thick.[7] AFM images of the films transferred to mica show the presence of a film a few layers thick and faceted crystallites about 10 layers thick. More recently,[8] GIXD and reflectivity studies of collapsed films of cholesterol have been interpreted in terms of a model in which there is a mixture of monolayer, a smooth bilayer, and a crystalline trilayer covered by a disordered monolayer.

The aim of this study is to examine the collapse of a Langmuir monolayer from a thermodynamic and structural point of view. We have focused on films of 10,12-pentacosadiyonic acid (PCA). Its phase diagram, structure, and elastic properties have recently been studied by detailed isotherm measurements, BAM imaging, and X-ray reflectivity, diffuse scattering, and GIXD experiments.[9] Here we examine the effects of temperature and compression rate on the isotherms and employ AFM and X-ray reflectivity to characterize the structures of the

* Corresponding author. E-mail: gourier@lps.ens.fr.
† Laboratoire de Physique de Statistique de l'Ecole Normale Supérieure.
‡ UCLA.
§ LURE.
|| CEA-Saclay.
⊥ Laboratoire de Dynamique des Fluides Complexes.

(1) See, for example: Ries, H. E., Jr. *Nature* **1979**, *281*, 287. Ries, H. E., Jr.; Kimball, W. A. *J. Phys. Chem.* **1955**, *59*, 94.
(2) Birdi, K. S.; Vu, D. T. *Langmuir* **1994**, *10*, 623.
(3) Vollhardt, D.; Kato, T.; Kawano, M. *J. Phys. Chem.* **1996**, *100*, 4141.
(4) Ramos, S.; Castillo, R. *J. Chem. Phys.* **1999**, *110*, 7021.
(5) Fang, J.; Dennin, M.; Knobler, C. M.; Godovsky, Yu. K.; Makarova, N. N.; Yokoyama, H. *J. Phys. Chem. B* **1997**, *101*, 3147. Buzin, A. I.; Godovsky, Yu. K.; Makarova, N. N.; Fang, J.; Wang, X.; Knobler, C. M. *J. Phys. Chem. B* **1999**, *103*, 11372.
(6) Ibn-Elhaj, M.; Riegler, H.; Möhwald, H.; Schwendler, M.; Helm, C. A. *Phys. Rev. E* **1997**, *56*, 1844.
(7) Lafonte, S.; Rapaport, H.; Sömjen, G. J.; Renault, A.; Howes, P. B.; Kjaer, K.; Als-Nielsen, J.; Leiserowitz, L.; Lahav, M. *J. Phys. Chem. B* **1998**, *102*, 761.
(8) Rapaport, H.; Kuzmemko, I.; Kjaer, K.; Howes, P. B.; Als-Nielsen, J.; Lahav, M.; Leiserowitz, L. *Biophys. J.* **2001**, *81*, 2729.
(9) Gourier, C.; Alba, M.; Braslau, A.; Daillant, J.; Goldmann, M.; Knobler, C. M.; Rieutord, F.; Zalczer, G. *Langmuir* **2001**, *17*, 6496.

10.1021/la026135v CCC: $22.00
Published on Web 10/30/2002

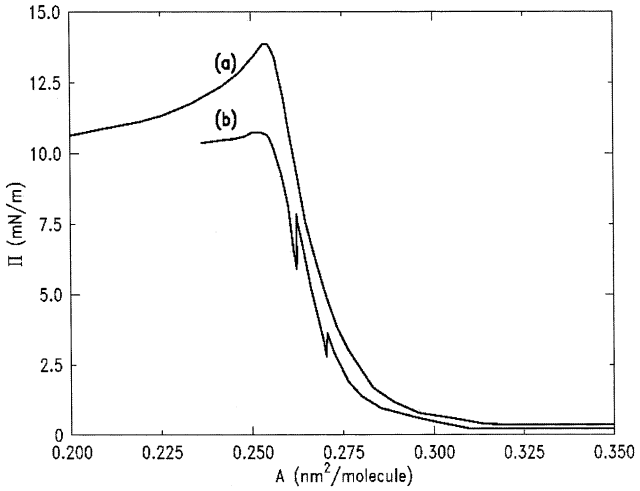

Figure 1. Pressure−area isotherms of PCA on pure water. The rate of compression was constant in isotherm a. The rate was the same in isotherm b, but the compression was stopped twice.

multilayer films that are formed. In light of the results obtained, we develop a mechanical description of the nucleation and growth of the collapsed domains.

Experimental Section

An extensive discussion of the sample preparation and details of the isotherm, imaging, and X-ray reflectivity measurements can be found in refs 9 and 10; we will therefore describe the procedures only very briefly.

The PCA, which was obtained from Lancaster, is easily polymerized, and the polymer had to be removed before each series of experiments. This was accomplished by filtration of hexane solutions. The monolayers were spread from solutions in 1:9 ethanol−hexane or chloroform. After preparation, solutions were stored in the dark at 5 °C. Isotherm and diffraction measurements were carried out in a 700 cm^2 homemade Teflon trough. Pressures were measured with a filter-paper Wilhelmy plate and an R&K transducer.

The AFM studies were performed on LB films with a Nanoscope II microscope (Digital Instruments) operated in contact mode. The force applied on the sample by the triangular silicon nitride tips was of the order of 1−10 nN.

LB transfers to silicon wafers were made in a 900 cm^2 Lauda trough at a transfer rate of 5 mm/min. The wafers had been cleaned in a hot sodium chromate/sulfuric acid bath for 30 min followed by repeated rinsing with Millipore water. They were then immersed in acetone in an ultrasonic bath. The acetone was allowed to evaporate in a laminar flow hood.

Reflectivity measurements were performed with a homemade laboratory diffractometer.[10] The source was a sealed tube with a copper cathode. A silicon monochromator was employed to select the $K\alpha_1$ line ($\lambda = 0.154$ nm). The real-space resolution fixed by the largest angle θ_{max} in the reflectivity curve was $\delta z = \lambda/4\theta_{max} = 0.9$ nm. This means that details larger than 0.9 nm are model independent. The use of known chemical information can give access to finer details.

Isotherm Measurements: Effects of Temperature and Compression Rate

As we noted earlier,[9] monolayers of PCA on a basic subphase are stable with respect to collapse, but those on pure water (pH = 5.5) are not. Nevertheless, pressure−area isotherms on pure water can be obtained by continuous compression, as shown in Figure 1. Isotherm a was measured by continuous compression; the compression in isotherm b was carried out at the same speed, but the barrier was stopped twice. The resulting drops in pressure are evident. It is necessary, then, to examine the behavior of the PCA films on water as a function not only of pressure and temperature but also of compression rate.

Pressure−area isotherms of PCA on pure water were measured in the temperature range 5.9 to 35 °C. In each case the amphiphile was spread from a 1:9 ethanol−hexane solution at a concentration of 1 mg/mL and compressed at a constant speed. (Reliable measurements could not be carried out at higher temperatures because evaporation of the subphase changed the zero of the Wilhelmy plate during the time of a compression and droplets of water that condensed on the cover of the trough fell into the subphase and carried impurities with them.) The isotherms are shown in Figure 2. At molecular areas that are consistent with a monolayer, the high-temperature isotherms display a plateau associated with an expanded−condensed transition (Figure 2b); the plateau is not evident below 29 °C (Figure 2a), which can therefore be taken as the triple point temperature at which the gaseous, expanded, and condensed phases are at equilibrium. The isotherms above the triple point are similar to those found for PCA on a basic subphase.[9] There are two major differences, however: (1) The rise in pressure preceding the expanded−condensed phase transition occurs at smaller areas (on the order of 0.55 nm^2/molecule on pure water compared to about 0.7 nm^2/molecule on a subphase at pH 7.5); (2) there is a shift to lower pressure of the expanded−condensed plateau. These differences are consistent with a decrease in the ionization of the headgroups at lower pH.

The collapse pressure depends on the rate of compression, as shown in Figure 3 for measurements of monolayers spread from chloroform solution at 20 °C in which the compression rates ranged from 0.056 to 5.6 cm^2/min. As shown in Figure 4, the collapse pressure varies linearly with the logarithm of the compression speed. This behavior is not typical of all monolayer collapse processes. For example, at the same temperature the collapse pressure of the liquid crystal 8CB, which is known to collapse to a trilayer,[2] shows no dependence on the compression rate (Figure 4). We interpret the low collapse pressure of PCA compared to that of simple fatty acids as being due to the polarizability of the acetylenic bonds, which might enhance the cohesion energy due to van der Waals forces. This is also consistent with the fact (see below) that we mainly observe trilayer domains since the inverse square distance dependence of the van der Waals energy should favor them on thicker domains.

The behavior of PCA films depends on the spreading solvent as well. For monolayers spread from 1:9 ethanol−hexane solutions (the 13 °C isotherms in Figure 5 are typical of the curves obtained), the peaks at collapse are more evident than those obtained with chloroform (Figure 3). We suspect that the differences are associated with the uniformity of spreading. Ethanol−hexane solutions spread more evenly across the surface than those prepared with chloroform, which leads to fewer defects and more uniform monolayers.

The influence of the temperature on the collapse behavior was studied with monolayers spread from ethanol−hexane. These results are summarized in Figure 6, a semilogarithmic plot of the plateau collapse pressure versus compression speed V for temperatures ranging from 0.5 to 27.5 °C. The data can be represented by an equation of the form

$$\pi = A(T) + B \log V \qquad (1)$$

(10) Bourdieu, L.; Chatenay, D.; Daillant, J.; Luzet, D. *J. Phys. II (France)* **1994**, *4*, 37.

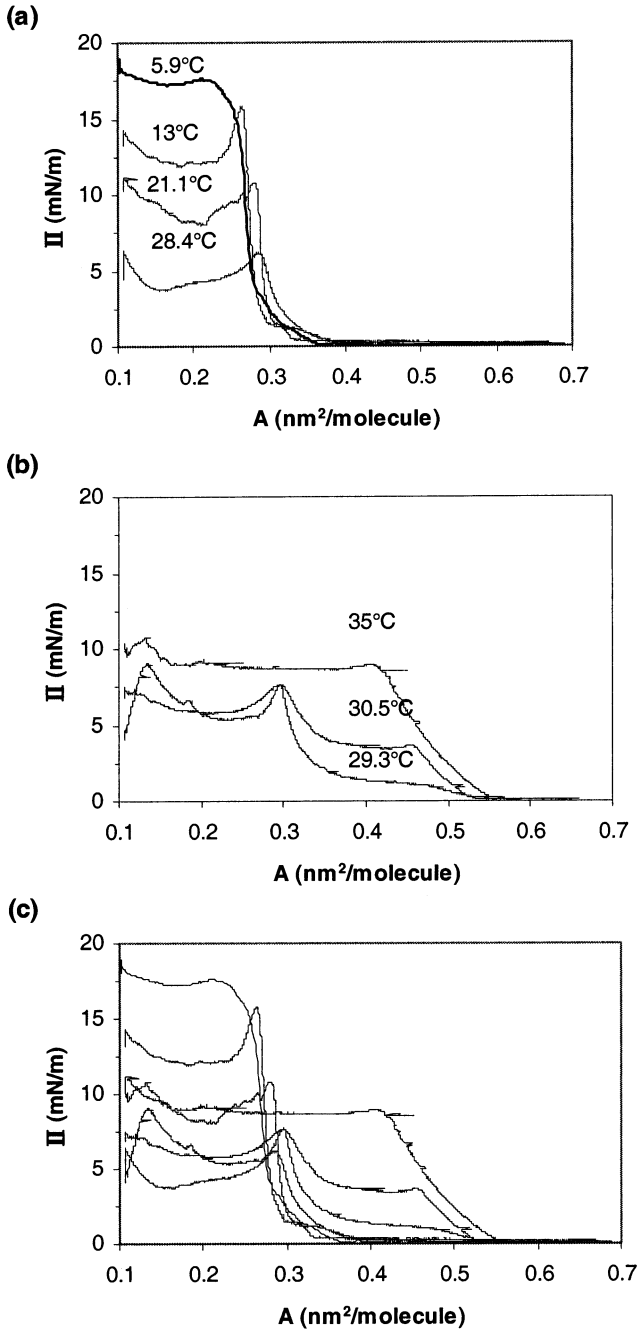

Figure 2. Pressure−area isotherms of PCA on pure water at different temperatures: (a) 5.9 °C < T < 29 °C; (b) T > 29 °C; (c) plots a and b superposed.

Over the 30 K range of the measurements, the intercept A decreases linearly by about a factor of 3 while B is constant (Figure 7).

AFM Measurements

To establish the properties of the condensed monolayer, LB transfers to silicon wafers were carried out by vertical dipping at a pressure < 0.1 mN/m and a molecular area of 0.7 nm^2. The films were imaged by AFM (Figure 8). As in the case of PCA monolayers on a basic subphase,[9] the film is heterogeneous under these conditions. The islands have a uniform height of 2.1 ± 0.2 nm, which is less than the length of a fully extended chain, 3.1 nm. The difference can be attributed to a molecular tilt of $\cos^{-1}(2.1/3.1) = 47°$ and/or disorder.

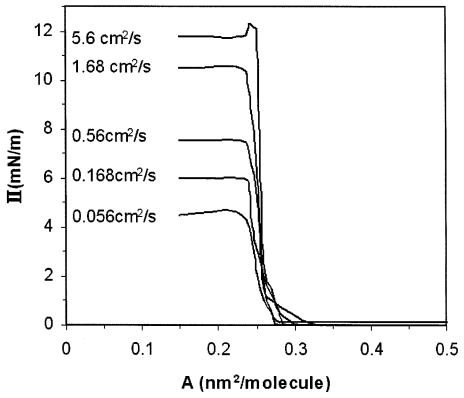

Figure 3. Effect of compression speed. The PCA was spread on pure water from chloroform solution at 20 °C.

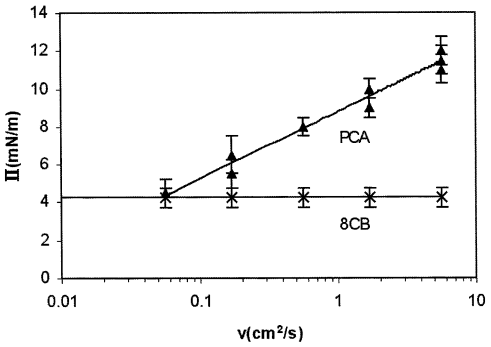

Figure 4. Dependence of the collapse plateau pressure on rate of compression for the PCA isotherms shown in Figure 3 and for 8CB on pure water.

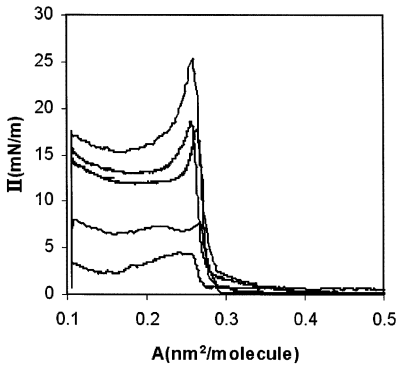

Figure 5. Effect of compression speed on PCA isotherms measured at 13 °C. The collapse pressure decreases when the compression speed increases. The PCA was spread from a 1:9 ethanol−hexane solution.

Transfers of the film compressed to a pressure of 5 mN/m and a molecular area of 0.28 nm^2 and then allowed to relax before the transfer were also performed (Figure 9). Under these conditions, we observe domains roughly rectangular in shape with sizes ranging from 5 to 500 μm^2 (Figure 9a and b). In light of the pressure relaxation shown in Figure 1, it would be reasonable to expect that the domains observed by AFM are multilayers on top of a monolayer of the condensed phase. When high forces were applied to the tip, however, the domains were easily deformed but the surrounding regions were unaffected (Figure 9c). We conclude that the domains rest on the silicon surface and not on a monolayer. The height of the domains is 5.1 ± 0.4 nm, which lies about midway between the heights of a bilayer and trilayer calculated from the AFM measurement of the monolayer.

Domains containing steps are observed in transfers made at much higher pressures, after the film has

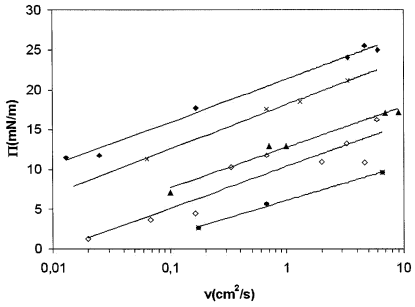

Figure 6. Variation of the peak pressure as a function of compression speed for temperatures between 0.5 and 27.5 °C.

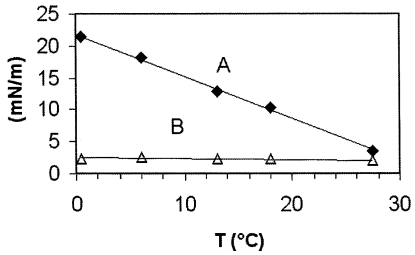

Figure 7. Dependence of the parameters *A* (squares) and *B* (triangles) of eq 1 on the temperature.

Figure 8. AFM images of a monolayer of PCA deposited on silicon at a pressure < 0.1mN/m and a molecular area of 0.7 nm^2. The image is 100 × 100 μm^2.

collapsed (Figure 9d). The height of the lowest step is 2.0 ± 0.2 nm, but succeeding steps are 4.0 ± 0.2 nm high, results consistent with a monolayer 2.0 nm high and steps composed of bilayers. The 5-nm domains seen at lower pressures most likely represent trilayers composed of a monolayer and a tilted or disordered bilayer.

Reflectivity Measurements

Although the AFM images seem to indicate the presence of a trilayer even at low pressures and large molecular areas, there is a possibility that the structure of the film changed during or after the LB transfer, as has been sometimes observed.[3] We therefore undertook reflectivity measurements at the air/water interface. The reflectivity curves are shown in Figure 10. Three studies were carried out. In the first the film was compressed to 3 mN/m and held at constant pressure throughout the run, which took 12 h. During this time the molecular area decreased from 0.29 to 0.22 nm^2. From the separation in q_Z between the minima in the reflectivity curve, it is evident that the film thickness is greater than one monolayer.

We attempted to fit the data to a box model of a bilayer but without success, as shown by the dashed line in Figure 10. Better results (full line) were obtained with the four-box model for a trilayer sketched in Figure 10. The parameters (relative electron density and height) of each box are listed in Table 1. The thickness of the film is 6.75 ± 0.20 nm.

Table 1. Fit Parameters Obtained from X-ray Reflectivity Measurements

	film compressed and maintained at 3 mN/m	film obtained by depositing crystals	film obtained by depositing a conc soltn
γ (mN/m)	70	73	73
$\rho_{alk}/\rho_{water} \pm 0.03$	0.98	0.95	0.98
$\rho_{t2}/\rho_c \pm 0.1$	1.2	1.47	0.96
$\rho_{t1}/\rho_{water} \pm 0.15$	1.07	1.4	1.07
$l_{alk2} \pm 0.2$ nm	2.2	2.2	1.9
$l_{t2} \pm 0.1$ nm	0.3	0.5	0.4
$l_{alk1} \pm 0.2$ nm	4.1	3.2	3.7
$l_{t1} \pm 0.1$ nm	0.15	0.2	0.1

Reflectivity measurements were also carried out on a film formed by depositing crystals of PCA on the water surface. During the experiment the pressure never exceeded 0.1 mN/m. In this case the reflectivity data are again consistent with a trilayer with a height of 6.1 ± 0.2 nm (Table 1). Finally we measured the reflectivity of a film produced by depositing 50 μL of a 1 mg/mL solution at an area of 120 cm^2, which corresponds to an average molecular area of 0.15 nm^2. Once again (Figure 9, Table 1), the film thickness was 6.4 ± 0.2 nm.

Mechanism of Collapse

Phenomenological Analysis. Our observations of the kinetics of collapse and the BAM and X-ray characterization of films that have collapsed can be compared with simple deductions about the mechanism obtained from consideration of the variation with time of the occupied film area, $S(t)$. In part, the arguments are similar to those used by Vollhardt and Retter.[11] We can write

$$S(t) = S_{2D}(t) + S_{3D}(t)$$

where S_{2D} is the area of the film that consists only of a monolayer and S_{3D} is the area that is covered by three-dimensional domains. If Γ is the molecular surface concentration within the 2D phase during the collapse transition, which remains constant because the collapse occurs at constant temperature and surface pressure, and N_{3D} is the number of molecules in the 3D phase, then

$$\frac{dS}{dt} = -\frac{1}{\Gamma}\frac{dN_{3D}}{dt} + \frac{dS_{3D}}{dt}$$

There are two contributions to the changes in S_{3D} with time: (1) the appearance of n^* nuclei of critical area S^*, which is given by $(dn^*/dt)S^*$, and (2) the growth of critical nuclei that have formed at an earlier time t', which can be calculated from $\int_0^t (dn^*/dt)_{t'}(dS_d/dt)_{(t-t')}\, dt'$. Here $(dS_d/dt)_{(t-t')}$ is the rate of growth of a nucleus of age $(t - t')$. One can use similar arguments to obtain an expression for dN_{3D}/dt, with dS_d/dt equal to the surface variation of a domain of age $(t - t')$, S^* the number of molecules in a nucleus, and dN_d/dt equal to the variation of the number of molecules in a domain of age $(t - t')$.

Thus, the change of S with time is the sum of four terms, two for nucleation and two for growth:

$$\frac{dS}{dt} = \frac{dn^*}{dt}S^* + \int_0^t \left(\frac{dn^*}{dt}\right)_{t'}\left(\frac{dS_d}{dt}\right)_{(t-t')} dt' - \frac{1}{\Gamma}\left[\frac{dn^*}{dt}N^* + \int_0^t \left(\frac{dn^*}{dt}\right)_{t'}\left(\frac{dN_d}{dt}\right)_{(t-t')} dt'\right] \quad (2)$$

In our experiments, during the collapse transition, dS/dt

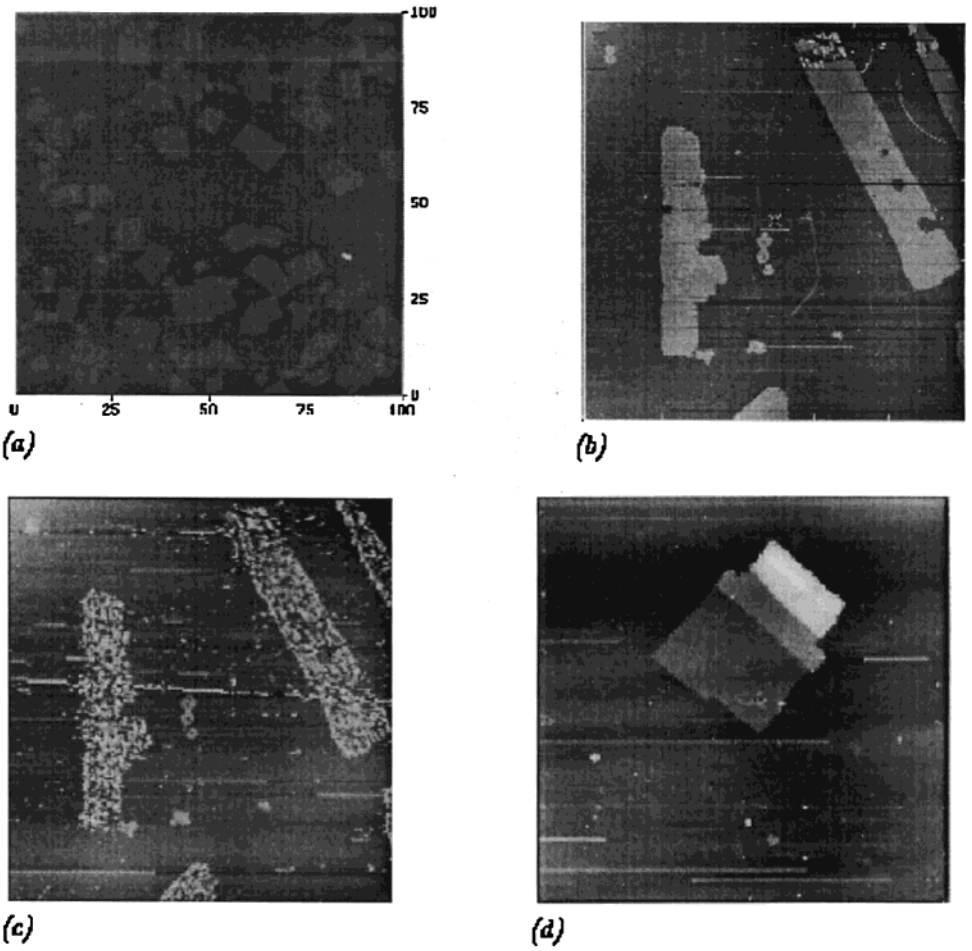

Figure 9. AFM images of (a−c) trilayers and (d) a multilayer of PCA deposited on silicon. The images are 100 × 100 μm^2.

is constant. Moreover, the pressure remains constant when chloroform (Figure 3) is used as spreading solvent and is approximately constant with the ethanol−hexane mixture (Figure 5). In that limit, which we only consider below, the terms in eq 2 must be either constant or zero, and if there are nonconstant terms, they must balance each other. Since we are dealing with nucleation and growth of multilayers, that is, $S^* < N^*/\Gamma$ and $dS_d/dt < 1/\Gamma\, dN_d/dt$, this latter possibility is excluded. We will therefore consider individually the different possible cases.

If dn^*/dt is constant, then $dS_d/dt = 0$, and $dN_d/dt = 0$. In this case no growth of the nucleus is possible. The different sizes of the domains observed on the AFM measurements show that this is not the case.

Another possibility is that the nucleation is effectively instantaneous, that is, dn^*/dt is nonzero only at $t = 0$ (this is also the case if collapse occurs from preexisting nuclei). Were this so, either $dS_d/dt = 0$ or dS_d/dt is constant and $dN_d/dt = 0$ or dN_d/dt is constant. If $dS_d/dt = 0$, the only growth mechanism possible is one in which the nuclei grow only vertically and not horizontally. The AFM measurements show that this is not the case, demonstrating that the growth cannot be only in the vertical direction. The condition $dS_d/dt = 0$ and $dN_d/dt = 0$ or dN_d/dt is constant must be excluded.

The condition dS_d/dt and dN_d/dt are constant is possible only if the domains are angular because a constant value implies that the growth occurs on an edge or on two opposing edges if there is a symmetry axis between them. Such anisotropic lateral growth may also be accompanied by vertical growth. This scenario is consistent with the more or less rectangular domains, with or without steps, that we have observed by AFM (Figure 6).

Dependence of the Collapse Pressure on Compression Rate. An influence of compression rate on collapse has been noted in a number of other studies.[12−15] Kwok et al.[12] examined collapse in monolayers of 1-octadecanol. Although they observed that the collapse pressure increased with increasing compression speed, a careful analysis showed that the effect was related to the initial surface concentration, which varied systematically in the studies. They argue that the collapse pressure depends on the number of defects in the monolayer. When more material is spread initially, the monolayer is more highly defected and collapses at a relatively low pressure. In essence, this is what we have seen in the dependence of the collapse pressure on the spreading solvent. This phenomenon cannot account for the relation between collapse pressure and compression speed that we have observed because in our experiments the amount of material initially spread was held constant.

The rate dependence of collapse in polymer monolayers has also attracted attention. For example, Adams et al.,[13] who measured pressure−area isotherms of a smectic liquid crystalline polymer, wrote the pressure along the collapse

(11) Vollhardt, D.; Retter, U. *J. Phys. Chem.* **1991**, *95*, 3723.

(12) Kwok, D. Y.; Tadros, B.; Deol, H.; Vollhardt, D.; Miller, R.; Cabrerizo-Vílchez, M. A.; Neumann, A. W. *Langmuir* **1996**, *12*, 1851.

(13) Adams, J.; Buske, A.; Duran, R. S. *Macromolecules* **1993**, *26*, 2871.

(14) Rapp, B.; Gruler, H. *Phys. Rev. A* **1990**, *42*, 2215.

(15) Kampf, J. P.; Frank, C. W.; Malmström, E. E.; Hawker, C. J. *Science* **1999**, *283*, 1730.

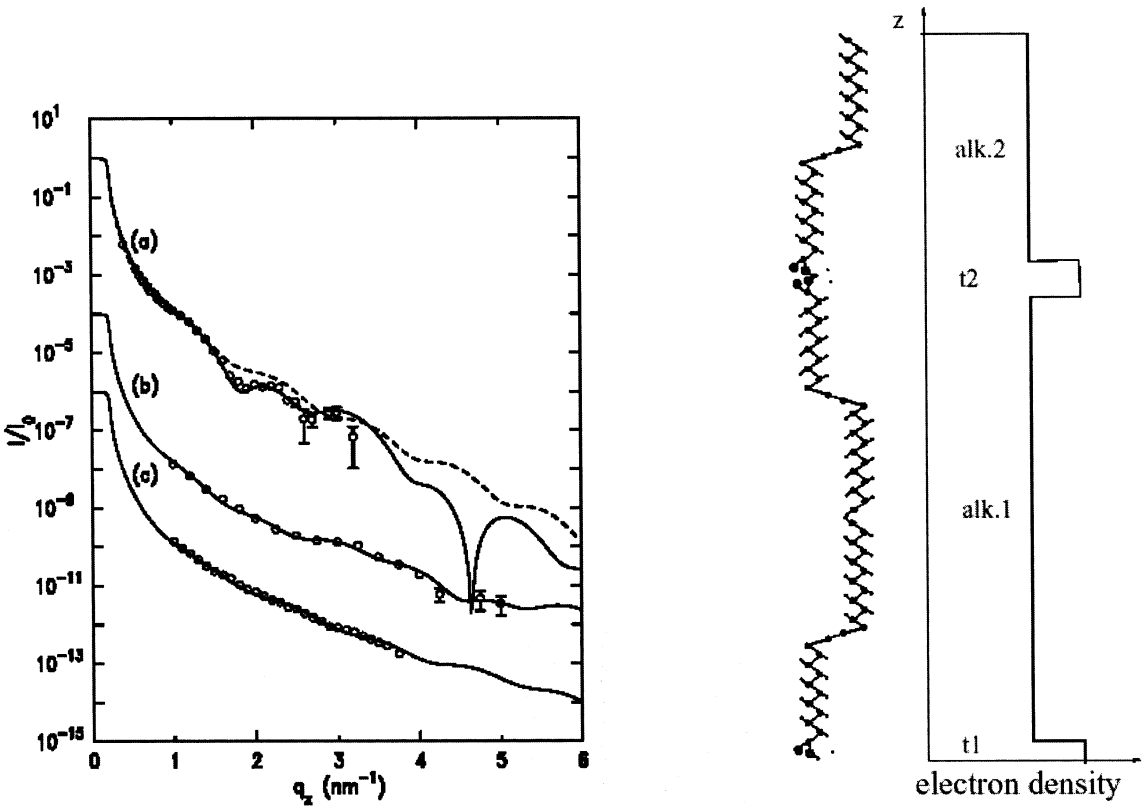

Figure 10. X-ray reflectivity of a PCA film on pure water (left) and model box for a trilayer (right). (a) Compressed to Π = 3 mN/m and maintained at constant pressure; (b) obtained by depositing crystals of PCA on the surface; (c) obtained by depositing a concentrated solution of PCA on pure water. For clarity the I/I_0 values of curves b and c have been divided by 10^4 and respectively 10^6. The dashed curve was calculated from a box model for a bilayer, and the full curve, from the trilayer box model shown on the right.

plateau as the sum of an equilibrium pressure and a dynamic "viscoelastic pressure", which they associated with the buildup of internal stresses.

Rapp and Gruler[14] studied the collapse of monolayers of the smectic liquid crystal HOBACPC (*p*-hexoxybenzylidene-*p*′-amino-2-chloro-α−propyl cinnamate), which occurs by a stepwise formation of layers. The collapse pressure increases linearly with the area compression rate. The constant of proportionality between the collapse pressure and speed, which has the dimensions of a viscosity, decreases by a factor of about two when the temperature is increased from 7 to 25 °C but then remains constant until 50 °C, the highest temperature studied. Since the data were taken over a range of speeds of only a factor of 6, it is difficult to distinguish a linear dependence from the logarithmic dependence that we have found. Indeed, we can fit their data within the experimental error by eq 1, but only if the coefficient B is taken as temperature dependent below 25 °C.

A qualitative similarity between the collapse behavior of monolayers and the stress−strain behavior of polymers subjected to tensile deformation has been noted by Kampf et al.[15] They applied equations that describe the mechanical response of bulk solids to the collapse of monolayers of highly branched polymers and obtained a power-law relation between the collapse pressure and the strain rate:

$$\pi = C\left(\frac{\mathrm{d}\alpha}{\mathrm{d}t}\right)^{\gamma}$$

where $\alpha = (1 - A(t)/A(t = 0))$ is the strain rate, C is a temperature-dependent constant, and $\gamma = 0.072$ for the system they have studied. The power-law behavior is demonstrated by the linearity of a log−log plot of π against α^{γ}. But the range of the measured collapse pressures is small, 7.2−8.6 mN m^{-1}, and plots of log π against log α^{γ} differ little from those of π against α^{γ}. Thus, eq 1 would fit the data equally well. As in the case of PCA, the collapse pressure decreases with increasing temperature.

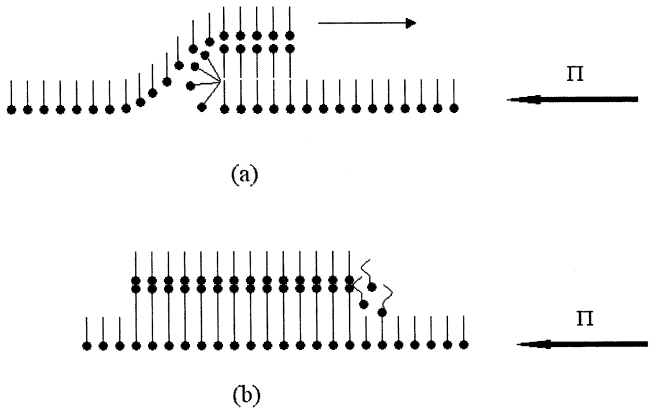

Figure 11. Processes by which a trilayer can grow from a monolayer: (a) folding of the monolayer and sliding between layers of the monolayer; (b) growth by the edge.

A logarithmic dependence of the collapse pressure is suggestive of an activation process. We can imagine two different processes by which a trilayer can grow from a monolayer (Figure 11). The first possibility is by direct trilayer growth at the edge. This process can be facilitated by the stress at the monolayer−trilayer border. This would imply the crossing of an activation barrier. The second possibility is by folding of the monolayer[16] and involves

(16) Nikomarov, E. S. *Langmuir* **1990**, *6*, 410.

the sliding between layers of the monolayer. Briscoe and Evans[17] measured the frictional force between two mica plates covered with LB monolayer films of fatty acids. For stearic acid, they observed that the shear stress τ (the frictional force divided by the contact area) varied logarithmically with velocity V at constant temperature and contact pressure:

$$\tau = \tau_0 + \theta \log V \tag{3}$$

They interpreted their observations in terms of an activated state model that leads to a linear decrease of τ_0 with temperature and a linear increase in θ. Thus, the forms of eqs 1 and 3 are identical and, like τ_0, A in eq 1 decreases with increasing temperature. Briscoe and Evans value for θ ($\theta = 0.42$ MPa) is in reasonable agreement with the B/h value ($B = 2.2 \pm 0.2$ mN/m, obtained from fitting curves of Figure 6, and $h \sim 2.6$ nm being the height of a monolayer deduced from Table 1) equal to 0.86 MPa. On the other hand, we do not observe any significant temperature dependence in the coefficient of the logarithmic term B. While more recent experiments[18,19] on frictional properties of monolayers show the shear stress is often linear in the ln V at low sliding velocities, in accord with eq 3, the temperature dependence of θ is not the simple monotonic variation suggested by Briscoe and Evans and it is effectively constant in some regions of temperature.

Conclusions

While the dynamic measurements might suggest a sliding mechanism for collapse, the AFM images do not show any evidence of folding and displacement of one portion of the monolayer with respect to another. Indeed, the regular shape of the domains suggests, in accord with the phenomenological analysis, that the domains grow by the diffusion along the surface. The process by which molecules are removed from the monolayer on the water surface is not at all clear, however, and it is with it that the compression speed dependence of pressure may be associated.

Acknowledgment. This work was sponsored in part by NATO and by the U.S. National Science Foundation (Grant CH007931). We are pleased to acknowledge fruitful discussions with Dr. Michel Alba, Dr. Alan Braslau, and Prof. Ian Peterson.

LA026135V

(17) Briscoe, B. J.; Evans, D. C. B. *Proc. R. Soc. London A* **1982**, *380*, 389.

(18) Yamada, S.; Israelachvili, J. *J. Phys. Chem.* **1998**, *102*, 234.

(19) Liu, Y.; Evans, D. F.; Song, Q.; Grainger, D. W. *Langmuir* **1996**, *12*, 1235.